Journal of Organometallic Chemistry, 331 (1987) 29–43
Elsevier Sequoia S.A., Lausanne – Printed in The Netherlands

Coordination chemistry of group 14 metalloles

IV *. Crystal structure and dynamic stereochemistry of *cis*-dicarbonyl-bis(η^4-1,1,3,4-tetramethylsilole)molybdenum and related complexes

Francis Carré, Ernest Colomer, Robert J.P. Corriu, Marc Lheureux

Laboratoire "Hétérochimie et Amino-Acides", U.A. CNRS 1097, Institut de Chimie Fine, Université des Sciences et Techniques du Languedoc, Place E. Bataillon, F-34060-Montpellier-Cédex (France)

and Adrien Cavé

Centre CNRS-INSERM de Pharmacologie-Endocrinologie, Rue de la Cardonille, B.P. 5055, F-34033 Montpellier-Cédex (France)

(Received February 19th, 1987)

Abstract

The crystal structure of *cis*-$Mo(CO)_2(\eta^4$-1,1,3,4-tetramethylsilole$)_2$ (**1**) shows the presence of only the *uu* isomer, as an enantiomeric pair (Δ, Λ). Variable temperature NMR measurements reveal the presence in solution of the Δ and Λ enantiomers (presumably *uu*) for the four *cis*-$M_T(CO)_2(\eta^4$-silole$)_2$ complexes, M_T = Mo (**1**, **6**), M_T = W (**2**) and *cis*-$Mo(CO)_2(\eta^4$-germole$)_2$ (**3**), but also the diastereoisomers ($\Delta\Lambda$ *uu* and *trans ou*) in the case of *cis*-$Mo(CO)(PPh_3)(\eta^4$-silole$)_2$ (**5**). IR spectroscopy confirms the presence of diastereoisomers for all the complexes and ^{31}P NMR also shows this in the case of **5**. The structures of the diastereoisomers are assigned on the basis of the multiplicity of the ^1H NMR signals. Both rotations of the η^4 ligands and classical twists, of the type usually associated with octahedral chelate complexes, are necessary to explain this dynamic behaviour fully. The activation parameters have been calculated and the values of 30–40 kJ mol^{-1} for ΔG^* at the coalescence temperature are comparable to those obtained for similar systems.

Introduction

We previously described the ability of siloles and germoles without phenyl substitution to act as ligands in transition metal chemistry [1,2] and showed that

* For Part III, see Ref. 2.

0022-328X/87/$03.50

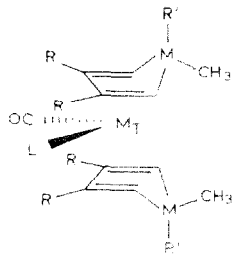

	M_T	M	R	R'	L
1	Mo	Si	CH_3	CH_3	CO
2	W	Si	CH_3	CH_3	CO
3	Mo	Ge	CH_3	CH_3	CO
4	Mo	Si	H	CH_3	CO
5	Mo	Si	H	CH_3	PPh_3
6	Mo	Si	CH_3	Ph	CO

Fig. 1. List of the complexes studied in this work.

they function as η^4 ligands, as is the case for the *C*-phenyl-substituted series [3]. Since silole transition metal complexes are of interest as potential sources of the still unknown η^5-silacyclopentadienyl species [4,5], a study of the electronic structure of these new complexes was carried out, a some aromatic character detected for the ligands [6].

The few crystal structures studied in the case of the *C*-phenylated series show that the silole ring is not planar [5,7]. Indeed, the roughly planar diene unit and the C(1)–Si–C(4) plane define dihedral angles of between 20 and 32°.

It thus seemed of interest to compare the structures of complexes of *C*- with those of non-phenylated siloles. We describe here the crystal structure of *cis*-dicarbonyl-bis(η^4-1,1,3,4-tetramethylsilole)molybdenum (**1**)) and the dynamic stereochemistry of this and related complexes: *cis*-$W(CO)_2(\eta^4$-1,1,3,4-Me_4silole$)_2$ (**2**), *cis*-$Mo(CO)_2(\eta^4$-1,1,3,4-Me_4germole$)_2$ (**3**), *cis*-$Mo(CO)_2(\eta^4$-1,1-Me_2silole$)_2$ (**4**), *cis*-$Mo(CO)(PPh_3)(\eta^4$-1,1-Me_2silole$)_2$ (**5**) and *cis*-$Mo(CO)_2(\eta^4$-1-Ph-1,3,4-Me_3silole$)_2$ (**6**) (Fig. 1).

Experimental

*Crystal structure of cis-dicarbonyl-bis(η^4-1,1,3,4-tetramethylsilacyclopentadiene)molybdenum (**1**). Crystal preparation*

Crystals of complex **1** were grown at −78°C from a hexane solution under nitrogen. Yellow blocks or truncated hexagonal plates were obtained. Preliminary Weissenberg photographs established a trigonal unit cell with space group $P_{\bar{3}c1}$ or P_{3c1} (nr. 158 and 165), systematic absences: $hh0l$ ($l = 2n + 1$). A small block was cut from a plate and was sealed inside a Lindeman glass capillary with the [001] direction parallel to the ϕ axis of the diffractometer.

Table 1

Summary of crystal data, intensity measurements, and refinement

Formula	$C_{18}H_{28}MoO_2Si_2$
Cryst. system	trigonal
Space group	$P\bar{3}c1$
a (Å)	16.491(3)
c (Å)	12.836(3)
Vol. (Å^3)	3022.8
Mol. wt	428.5
Z	6
d_{calcd} (g cm^{-3})	1.414
d_{measd} (g cm^{-3})	1.35(2)
Cryst. size (mm^3)	$0.15 \times 0.20 \times 0.25$
Cryst. colour	yellow
Recrystn. solv	hexane
M.p. (°C)	91–92
Method of data collectn	moving crystal, moving counter
Radiatn (graphite-monochromated)	Mo-K_α
μ (cm^{-1})	6.92
2θ limits (deg)	4–50
No. of unique reflectns	1677
No. of obsd reflectns	1184
Final no. of variables	105
R	0.0416
Rw	0.0437
Residual electron density	0.67

X-Ray data collection

Data were collected on a CAD-4 automated diffractometer with graphite-monochromatized Mo-K_α radiation (λ 0.71069 Å). Lattice constants (Table 1) were derived from a least-squares refinement of 25 strong reflections recorded in the range $12° < 2\theta < 25.6°$. The intensities of three standard reflections were monitored at 60 min intervals, and no changes were observed. The structure amplitudes were obtained after the usual Lorentz and polarization reduction. From the 3913 data collected, equivalent pairs were averaged and the absent reflections deleted to give a set of 1677 unique data, of which only 1184 were used in the last refinement ($\sigma(F)/F < 0.33$). Since the crystal was small and the linear absorption coefficient only 6.9 cm^{-1}, no absorption corrections were made.

Structure determination and refinement

The space group P_{3c1} was first tried and the structure was solved by direct methods (1980 version of the MULTAN program). The Mo coordinates thus obtained were used in a Fourier map calculation, leading to location of all the non-hydrogen atoms. The atomic scattering factors were taken from ref. 8. After 4 cycles of least-squares refinement, Professor Lapasset pointed out to us that the molecule of complex **1** exhibits a rigorous 2-fold axis of symmetry (going through the Mo atom and bisecting the OC–Mo–CO angle). The coordinates of the atoms were changed leading to the centric space group $P_{\bar{3}c1}$ which was used successfully throughout the subsequent refinement cycles. Anisotropic thermal parameters were given to all atoms, the restrictions due to the special position in the case of the Mo

Table 2

Fractional atomic coordinates ($\times 10^4$) for complex **1**

Atom	x/a	y/b	z/c
Mo	3675.7(5)	0	2500
Si	2863.3(15)	1196.2(14)	3441.6(17)
C(1)	3289(6)	1221(5)	2092(6)
C(2)	4277(5)	1606(4)	2194(6)
C(3)	4557(5)	1444(5)	3202(6)
C(4)	3780(5)	935(5)	3907(6)
C	4744(6)	355(6)	1601(7)
O	5411(5)	524(5)	1086(6)
C(5)	4944(6)	2221(6)	1362(7)
C(6)	5578(5)	1872(6)	3543(7)
C(7)	1610(6)	406(6)	3782(7)
C(8)	3131(7)	2416(6)	3856(7)

atom being taken into account. The scale factor and the positional and thermal atomic parameters were refined by minimizing the function $\Sigma w(|F_o| - |F_c|)^2$, where $w = 1/(\sigma^2(F) + 0.0044F^2)$. The residuals R and R_w appear in Table 1, along with the residual electron density.

The final atomic coordinates are listed in Table 2. The labelling scheme is given in Fig. 2. Individual bond lengths and important bond angles are listed in Table 3. Thermal parameters and a list of observed and calculated structure factors are available from the authors.

NMR spectrometry

NMR spectra were recorded on a Bruker WM 360 WB. Chemical shifts, δ, are relative to TMS (int.) or to H_3PO_4 (ext.). Syntheses of complexes **1**–**5** are described in ref. 2. Complex **6** was prepared in the same manner as **1**, and detailed synthesis and properties will be described elsewhere [9].

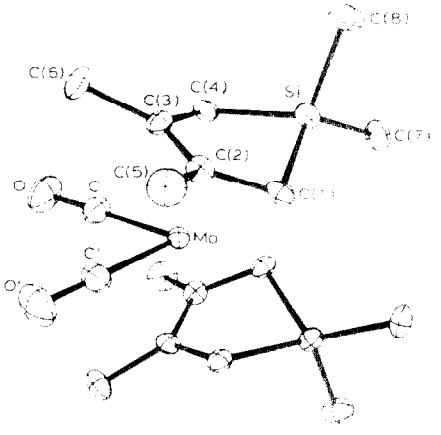

Fig. 2. General view of the molecule of complex **1** showing the labelling scheme and the 30% probability thermal ellipsoids.

Table 3

Bond lengths (Å) and selected bond angles (deg) for complex **1**, with standard deviations in parentheses

Mo–C(1)	2.454(10)	Si–C(7)	1.861(8)
Mo–C(2)	2.351(6)	Si–C(8)	1.907(10)
Mo–C(3)	2.265(7)		
Mo–C(4)	2.324(8)	C(1)–C(2)	1.428(11)
Mo–C	1.935(9)	C(2)–C(3)	1.442(12)
C–O	1.191(13)	C(3)–C(4)	1.445(10)
		C(2)–C(5)	1.504(11)
Si–C(1)	1.861(8)	C(3)–C(6)	1.528(11)
Si–C(4)	1.865(10)		
C–Mo–C′ [a]	81.2(6)	Si–C(1)–C(2)	105.0(5)
Mo–C–O	175.0(8)	C(1)–C(2)–C(3)	113.6(6)
		C(2)–C(3)–C(4)	113.3(7)
C(1)–Si–C(4)	87.8(4)	C(3)–C(4)–Si	104.6(6)
C(1)–Si–C(7)	120.5(4)		
C(1)–Si–C(8)	110.5(4)	C(5)–C(2)–C(1)	121.5(7)
C(4)–Si–C(7)	120.5(4)	C(5)–C(2)–C(3)	124.5(7)
C(4)–Si–C(8)	111.6(4)	C(6)–C(3)–C(4)	122.8(7)
C(7)–Si–C(8)	105.3(5)	C(6)–C(3)–C(2)	123.5(6)

[a] Atom C′ is obtained from atom C through the symmetry transformation: $x-y$, $\bar{y}$, $1/2-z$.

Table 4

Variable temperature spectra of compounds **1–3** and **6** in CD_2Cl_2

Compound	T (K)	δ (ppm)			
		=C-CH_3	=C-H	*endo*-CH_3	*exo*-CH_3
1	300	2.31	1.71	0.31	−0.14
1	168	2.43, 2.08	2.12, 1.19	0.21	−0.24
2	300	2.49	1.44	0.34	−0.14
2	168	2.54, 2.26	1.74, 0.92	0.22	−0.23
3	300	2.40	2.02	0.52	0.06
3	183	2.49, 2.09	2.42, 1.39	0.39	−0.03
6	300	2.37	1.96	0.69	7.2–7.4 [a]
6	173	2.55, 2.11	2.38, 1.36	0.63	

[a] Aromatic.

Table 4 summarizes the results of variable temperature measures for compounds **1–3** and **6**.

Complex **5**: ^{1}H NMR, T 300 K, (CD_2Cl_2) δ 7.3–7.4 (m, aromatic), 5.09 and 4.24

Table 5

Coalescence temperatures and activation parameters for compounds **1**, **2**, **3** and **6**

Compound	T_c (=C-H) (K)	$T_c(CH_3)$ (K)	$\Delta\nu$(c,d) (Hz)	$\Delta\nu$(e,f) (Hz)	$\Delta G^{\star}_{T_c}$ (kJ mol^{-1})	$\Delta S^{\star}_{T_c}$ (J mol^{-1} K^{-1})	$\Delta H^{\star}_{T_c}$ (kJ mol^{-1})
1	183	178	335	142	34	−12	33
2	178	173	300	108	33	−80	22
3	208	198	371	143	38	−5	37
6	193	188	371	162	36	−17	32

(m, =C-H β to Si), 1.83 and 1.26 (m, =C-H α to Si), 0.49 (s, *endo*-CH_3) and −0.17 (s, *exo*-CH_3); *T* 173 K, δ 6.08, 5.62 (2 signals), 4.57, 4.22, 3.71, 3.43, 2.78, 2.48, 2.17, 1.91 and 1.00 (all broad singlets, preventing firm assignments, α and β to silicon), 0.86, 0.48, 0.28, 0.03, (s, *endo*-CH_3) and −0.16 (2 signals), −0.33 and −0.42 (s, *exo*-CH_3).

Coalescence temperatures and activation parameters for compounds **1**–**3** and **6** are listed in Table 5. They were calculated by use of the Eyring's equation [10]. For complex **5**, coalescence temperatures and activation parameters cannot be calculated from ^{1}H NMR data because of the complexity of the spectrum. From ^{31}P NMR: T_c 210 K, $\Delta G^{\ddagger}_{T_c}$ ~ 37 kJ mol^{-1}.

Results and discussion

*Crystallographic study of cis-dicarbonyl-bis(η^4-1,1,3,4-tetramethylsilacyclopentadiene)-molybdenum (**1**)*

The computer-drawn model displayed in Fig. 2 shows the essential features of the disilole molybdenum complex. The molecule has C_2 symmetry, with the axis bisecting the OC–Mo–CO angle, as can best be seen in Fig. 3. The same type of symmetry was observed by Kreiter [11] for $W(CO)_2(CH_2{=}CH\text{-}CH{=}CH_2)_2$. The four carbon–carbon double bonds and the two carbonyl groups are linked to the molybdenum atom in a octahedral arrangement, with deformations due to the vicinity of pairs of C=C ligands inside each silole ring. The carbonyl groups close together slightly (OC–Mo–CO angle: 81.2(6)°). No group or ligand can really be considered to lie *trans* to another ligand: the largest angle at the Mo atom, for instance, is C(3)–Mo–C′(3): 166.7(5)°, and the 'best' sp^2 carbon atom linked opposite to a carbonyl group is C(1), with a C(1)–Mo–C′ angle value of 145.3(3)°.

The fairly planar [12 *] diene unit C(1)–C(2)–C(3)–C(4) and the C(1)–Si–C(4) plane make a dihedral angle of ca. 36.6°, a value close to that recently observed for $Cr(CO)_4(\eta^4$-1,1,3,4-Me_4silole) [13], so that the silicon atom lies 0.80 Å from the butadiene plane on the side away from the Mo atom. As a consequence, the Mo · · · Si distance is 3.128(2) Å. This value for the fold angle is the largest observed in our group. Two other molybdenum tricarbonyl complexes [14] have angles of 9 and 28°, and one of 32° was reported by Muir [7] for the 2,5-diphenylsilole complex with tricarbonylruthenium. However, very high fold angle values (41.2 and

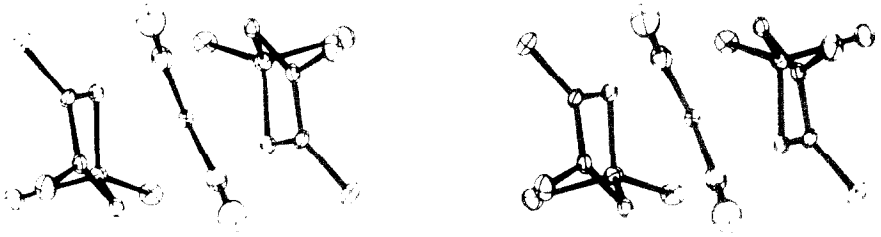

Fig. 3. Stereoscopic drawing of the molecule of complex **1** viewed down the C_2 axis. Ellipsoids are at the 20% probability level.

* Reference number with asterisk indicates a note in the list of references.

Table 6

Van der Waals contacts between groups within a molecule of complex **1**

C(sp)---C(sp^2)	Distance (Å)	C(sp)---C(sp^3)	Distance (Å)
C---C(2)	2.65(1)	C---C(5) (CH_3)	2.94(2)
C---C(3)	2.84(1)	C---C′(6) (CH_3)	3.19(1)
C---C′(3)	2.85(1)	C---C(6) (CH_3)	3.30(1)
C---C′(4)	2.85(1)	C(7)---C′(7) (CH_3---CH_3)	3.49(2)

44.5°) have been reported recently [15] for silole and germole cobalt complexes. We think that the larger fold angle for the silole ring in complex **1** results from a greater compression associated with the presence of more ligands around the molybdenum atom. In the case of $Ru(CO)_3$(1,1-Me_2-2,5-Ph_2silole) [7] or $Mo(CO)_3$(1-Me-1-vinyl-2,5-Ph_2silole) and $Mo(CO)_3$(1-Me-1-allyl-2,5-Ph_2silole) [14], the $Ru(CO)_3$ or the $Mo(CO)_3$[C=C] moieties readily occupy the space left by the unique silole ligand. In the present work, the two carbonyl groups are linked to the Mo atom in a way which is reminiscent of the octahedral geometry, and so they cannot define a plane which contains the metal atom and is perpendicular to a line joining the two silole ring centers, a situation which would have minimized steric interactions. On the contrary, as can be seen from Table 6, the carbon atoms in the carbonyl groups and the Van der Waals sphere of methyl group C(7) are in close contact with their neighbours.

Another possible effect of the asymmetric repulsions reported in Table 6 may be the slight rotation of the silole ligand around an axis going approximatively through the C(2) and C(4) atoms. Thus Mo–C(1) bond distances, that are usually observed as equivalent pairs (e.g. Mo–C(1), C(4) and Mo–C(2),C(3)), are in this case significantly different: the Mo–C(1) bond distance is 0.13(1) Å greater than the corresponding Mo–C(4) distance, and the Mo–C(2) and Mo–C(3) distances differ by 0.09(1) Å. This dissymmetry in the coordination of the molybdenum atom to the butadiene unit leads to slight different values for the carbon–carbon bond lengths of the silole rings: C(1)–C(2) is 0.015 Å shorter than the average of the two C(2)–C(3) and C(3)–C(4) bond lengths, although such small differences fall within the range of experimental error. However, the overall magnitude of these steric repulsions must be small, since the Mo atom in complex **1** is closer to the butadiene unit (average Mo–C distance: 2.348(7) Å) than in the complexes $Mo(CO)_3$(1-Me-1-vinyl-2,5-Ph_2silole) 2.402(7) Å and $Mo(CO)_3$(1-Me-allyl-2,5-Ph_2silole) (2.369(7) Å) [14].

Spectroscopic study of bis-metallole molybdenum and tungsten complexes

From the crystal structure of **1**, a magnetic non-equivalence would be expected for the olefinic protons c and d and the methyl protons e and f, since their chemical environments are different (Fig. 4). The ^1H NMR spectrum exhibits sharp singlets for each type of protons [2] showing that there is interconversion in solution. However, at lower temperature there is decoalescence (T_c 183 K for c and d, T_c 178 K for e and f). The measured $\Delta\nu$ at 168 K are 335 and 142 Hz, respectively (Fig. 5).

The same behaviour is displayed by compounds **2**, **3** and **6** (Fig. 1), the structures of which are assumed to be like that of **1**. From these experiments, the values ΔG,

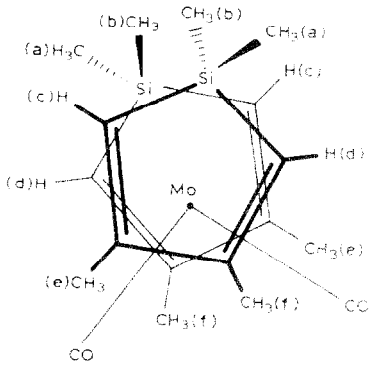

Fig. 4. Schematic view of complex **1** showing the magnetic non-equivalence of protons.

ΔS and ΔH of activation at the temperature of coalescence can be calculated (Table 5).

Complex **5** possesses a single ^{31}P resonance at δ 70 ppm at 278 K while at 210 K a decoalescence occurs. At 172 K two different signals are observed (δ 72 and 68 ppm) with relative ratios 3/2. For this process $\Delta G^{\star}_{T_c} \sim 37$ kJ mol^{-1}, a close value to $\Delta G^{\star}$ for the interconversion, in compounds **1**–**3**. Its ^1H NMR spectrum consists in

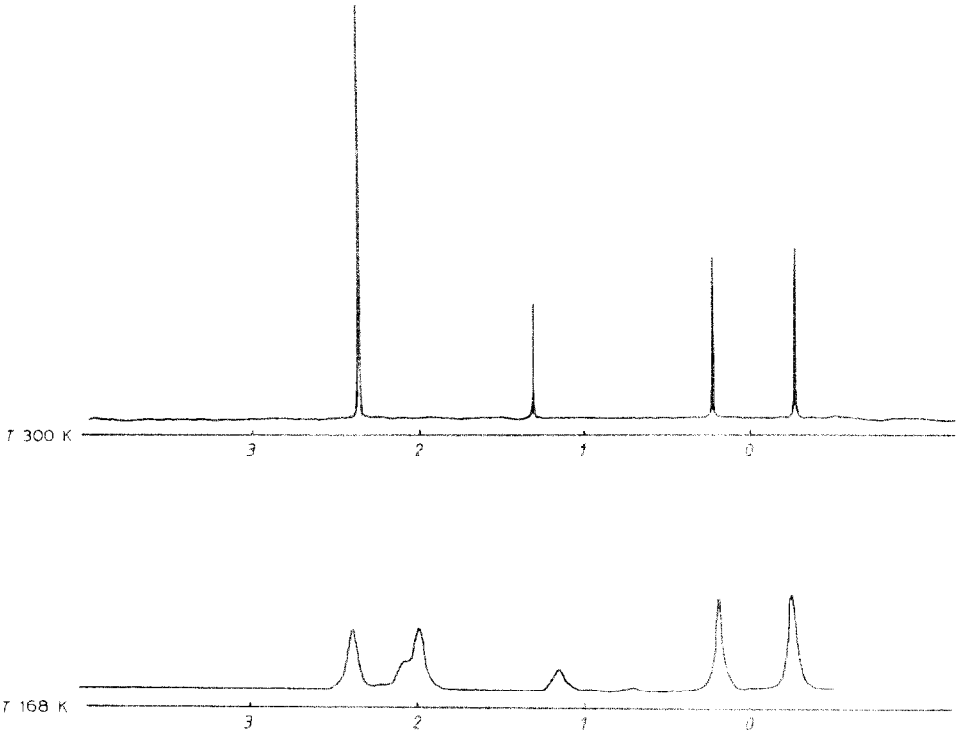

Fig. 5. ^1H NMR spectra of **1** at room and low temperature.

Table 7

Carbonyl frequencies for compounds **1–6** in hexane (sh = shoulder)

Compound	ν(CO) (cm^{-1})
1	1978, 1972, 1919, 1912
2	1976, 1970, 1917, 1908
3	1970, 1963, 1912, 1905
4 [a]	2000sh, 1990, 1955sh, 1940
5 [a]	1916, 1890
6	1975, 1972, 1918, 1912

[a] In cyclohexane.

two multiplets for each type of protons (α and β to silicon) and two singlets (*endo* and *exo* methyls) at 298 K. From 223 to 183 K, the different signals decoalesce and at 173 K, the spectrum shows 12 signals for the olefinic protons and 8 for the methyl protons. The results can be related to our previous observations [2] on the IR spectra of these complexes; in each case the ν(CO) absorptions show a multiplicity which is the double than that predicted (Table 7).

Our observations are consistent with the coexistence of isomers which undergo rapidly interconversion on the NMR time scale at room temperature; the process is slower at low temperature and so for complex **1**, the non-equivalence of protons evident in the crystal structure, is observed. The equivalence observed at higher temperatures is the result of the equilibrium between the enantiomers (Fig. 6). Enantiomers of a compound have identical physical properties except that the angle of rotation of the plane of polarized light has the opposite sign. Thus, the observed ν(CO) bonds correspond to two diastereoisomers. Diastereoisomers are not observed for either the ^{1}H or ^{13}C spectra of complexes **1–3**, but the ^{31}P NMR spectrum of **5** is consistent with an interconversion of diastereoisomers since their populations are different (60 and 40%). Indeed, diastereoisomers are different chemical compounds, and their ratio at equilibrium should be different. On the basis of the crystal structure of **1**, one of the diastereoisomers must be **A** (Fig. 7). Whether the other is **B–F** can be deduced from the ^{1}H NMR spectrum (Fig. 8).

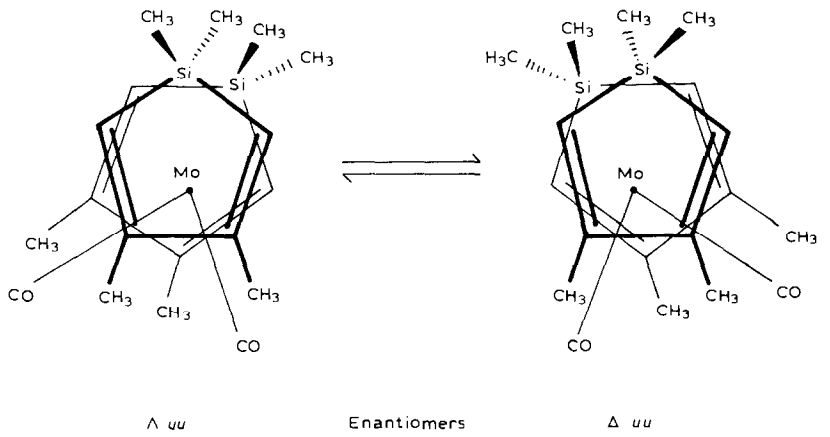

Fig. 6. Interpretation of the low temperature ^{1}H NMR of **1**.

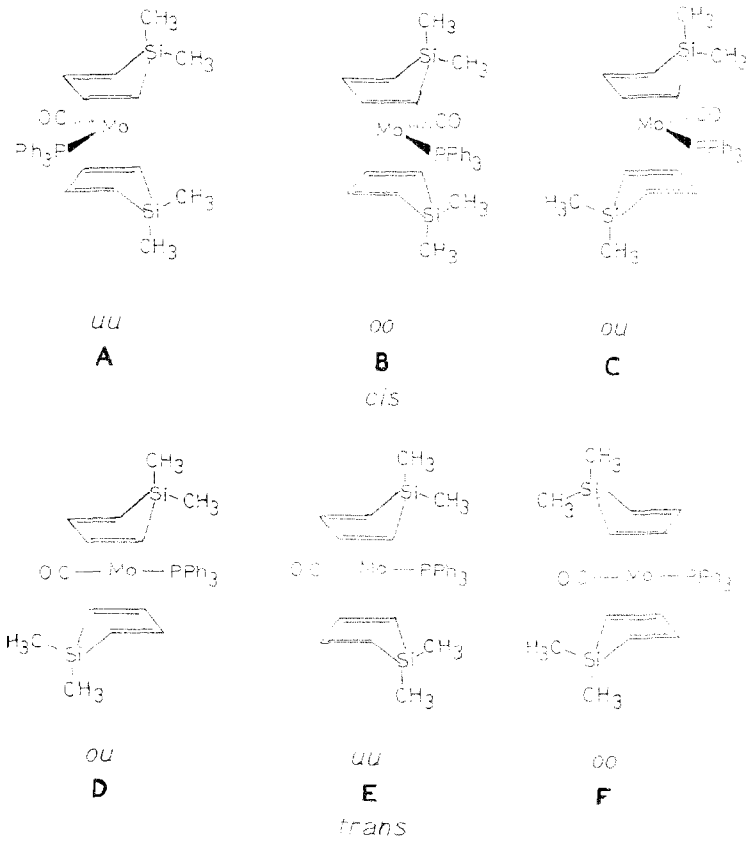

Fig. 7. Possible diastereoisomers of **5**.

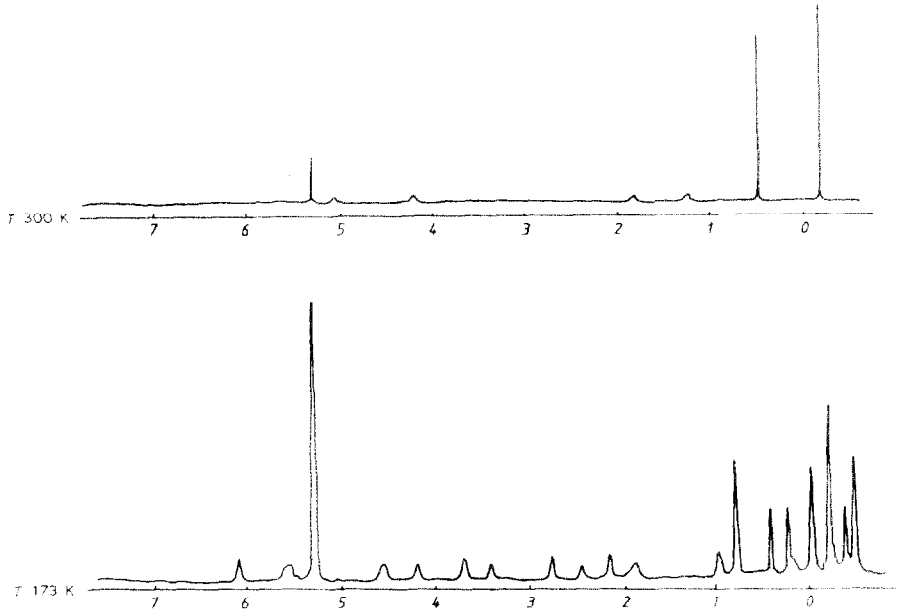

Fig. 8. ^{1}H NMR spectra of **5** at room and low temperature.

Above the coalescence temperature, the observation of two signals for the methyl protons and four for the olefinic ones is easily explained in terms of the interconversion of the Δ and Λ *uu* isomers (**A**). (The mechanism will be discussed below). Below the coalescence temperature, the observation of 12 signals (6 protons β and 6 protons α to silicon) rules out the equilibrium between two *cis* isomers (16 signals should be obtained in this case), as well as the equilibrium between **A** and **E** or **F** (10 signals should only be observed). The possibility of an equilibrium between **A**, **E** and **F** would be in agreement with the ^{1}H NMR spectrum, but not with the IR spectrum or with the low temperature ^{31}P NMR spectrum (only two diastereoisomers are present). Thus only the presence of one *cis* enantiomeric pair $\Delta\Lambda$ *uu*, presumably (**A**) and *trans ou* (**D**) is consistent with both the 12 signals due to the olefinic protons and the 8 due to the methyl protons.

Proposed mechanism for the isomerization of bis-metallole transition metal complexes

Since the crystal structure determination shows that **1** is a slightly distorted octahedral molecule, the recognised mechanisms for the isomerization of this type of compounds can be considered viz. bond rupture, twisting mechanisms [16–18], or dienic ligand rotation [19]. Dissociative mechanisms are difficult to rule out for complexes with one or more bidentate ligands [20], but the absence of signals other than those attributed to isomers **A** and **D** (Fig. 7) in the low temperature ^{1}H NMR spectrum of **5** favours a concerted rather than a bond rupture mechanism. Non-dissociative pathways to a transition state with a trigonal prism geometry from an octahedral ground state have been proposed. Our observations are in agreement with an intramolecular non-dissociative process which can be described as a Bailar [21], a Ray–Dutt [22], or a Springer–Sievers [23] twist. Such twists could explain the observation of an enantiomeric pair (complexes **1–3**) and signals which can be attributed to the enantiomeric pair and diastereoisomer **B** (complex **5**) (Fig. 9). However, the room temperature ^{1}H NMR spectrum of **5** cannot be rationalized in terms of a twist mechanism, since in this case the populations of the methyl protons should be always different and four signals would be observed (Fig. 10). In contrast, rotation of the silole ligands around an axis defined roughly by the gravity centers of the diene units would be consistent with the observation of only two resonances for the methyl protons. The same considerations apply to the olefinic protons in

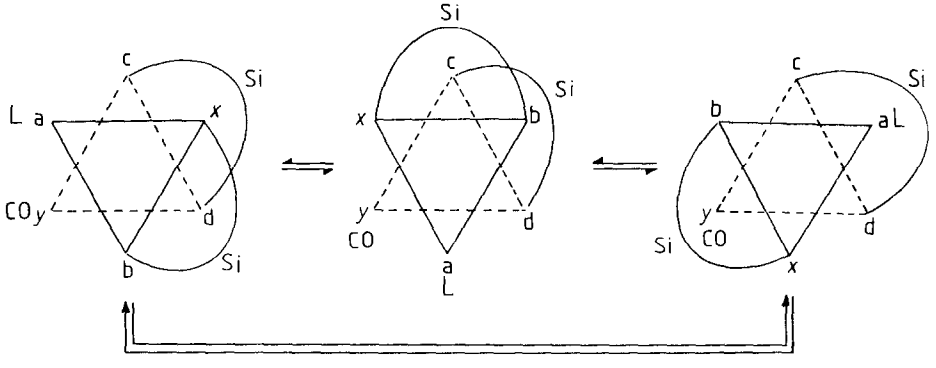

Fig. 9. Mechanism proposed for the isomerization of **5**.

Table 8

Double irradiation experiments on **5** at 173 K

Irradiated signal [a]	Reduction of the signal intensity (%)										
	O	P+Q	R	S	T	U	V	W	X	Y	Z
O	(100)	(69)	17	14	8	17	14	18	11	13	–
P+Q	(70)	(100)	20	20	(55)	15	23	20	17	15	15
R	14	20	(100)	8	14	(85)	8	–	8	12	18
S	10	10	10	(100)	18	12	(75)	–	5	8	10
T	5	(54)	16	18	(100)	18	23	–	5	19	–
U	12	15	(61)	9	16	(100)	12	–	11	11	9
V	11	–	6	(75)	16	7	(100)	10	11	9	9
W	12	14	7	8	–	8	9	(100)	(77)	9	6
X	–	14	5	6	6	8	10	(81)	(100)	12	8
Y	9	10	14	10	18	13	13	13	17	(100)	(77)
δ(ppm)	6.08	5.62	4.57	4.22	3.71	3.43	2.78	2.48	2.17	1.91	1.00

[a] Attributions are not given. In brackets, signals which are associated: (O,P), (Q,T), (R,U), (S,V), (W,X), (Y,Z).

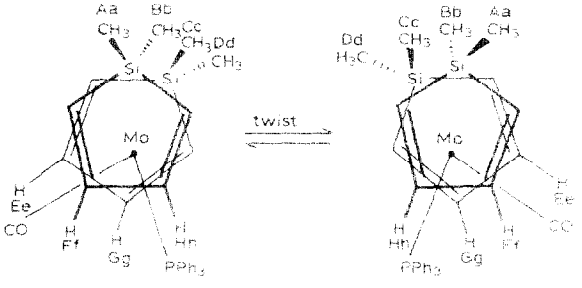

Molecular twist

The H populations for *endo*- and *exo*-methyls are all different. (Also for olefinic protons α and β to Si.)

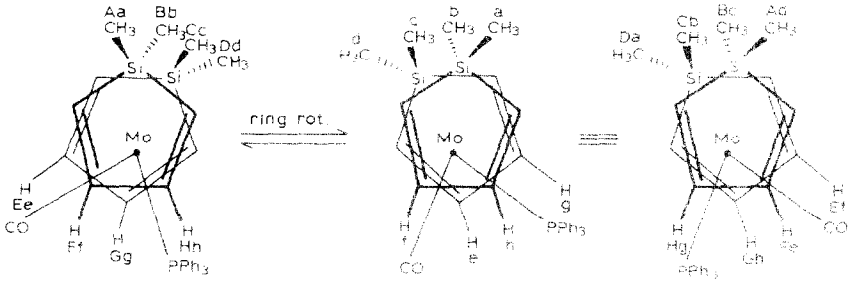

Ring rotation

The H populations for the *exo*-methyls are the same. (Also for the *endo*-ones and olefinic protons α and β to Si.)

Capital letters refer to chemical environments and lower case ones to populations.

Fig. 10. Possible molecular motions for complex **5**. (Olefinic protons α to Si omitted for simplicity).

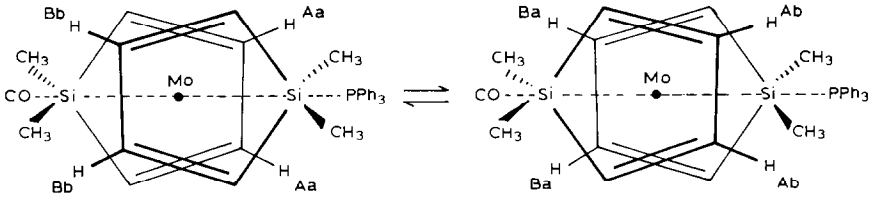

Fig. 11. Ring rotation in isomer *trans-ou* of complex **5**.

both mechanisms, only a ring rotation accounting satisfactorily for the multiplicity of the signals. Double irradiation experiments on the low temperature ^{1}H NMR spectrum of **5** show that each proton is associated with another (Table 8). This is also consistent with ring rotations in *cis-uu* (**A**) and *trans-ou* (**D**) isomers (Figs. 10 and 11), and shows that the energy of the protons is transferred in the ring rotation mechanism but not in the twist process; in other words, the twist is slow and the ring rotation fast in the proton relaxation time scale. The absence of other possible isomers is due to the constraints arising from the geometry of the η^4-bonding of the metallole ligands, which prevent twists such as those shown in Fig. 12, and also by steric hindrance, which prevents ring rotations. This reflects the limitations in comparing the isomerization of these complexes with those possessing only non-chelating or chelate ligands; the latter can undergo isomerizations forbidden by η^4-bonding.

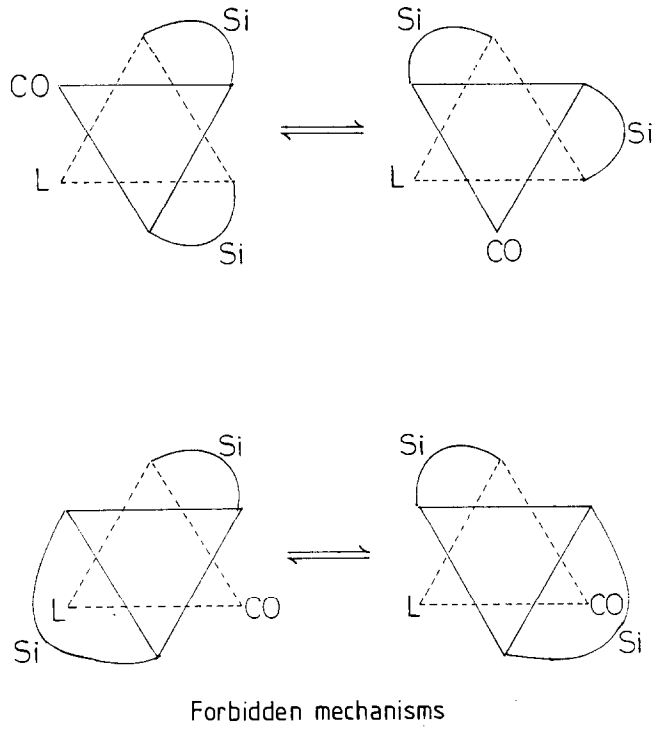

Fig. 12. Other formal possibilities of isomerization.

Fig. 13. Comparative view of $(butadiene)_2W(CO)_2$ and $(silole)_2Mo(CO)_2$.

Conclusion

Only one diastereoisomer of **1** is present in the crystal, but two are present in solution. This is reflected in the IR spectra in solution, and shown unambiguously by the variable temperature ^1H NMR experiments on complex **5**. Not all the possible isomers are observed, but only those that do not involve steric hindrance. The multiplicity of the spectrum of **5** under the coalescence temperature is compatible with the equilibrium **A** ⇌ **D** and eliminates the other *cis* and *trans* isomers.

The dynamics of quasi-octahedral η^4-diene metal complexes have been extensively studied by Kreiter and coworkers [19,24], who demonstrated their fluxionality. Some differences, however, are observed between these complexes and the metallole ones, and these can be attributed to steric restrictions due to the presence of the $M(CH_3)_2$ (M = Si, Ge) group in the latter; the former has the *oo* configuration, whereas the latter has the *uu* one (Fig. 13).

Both mechanisms (ring rotation and twist) can account for the results observed for the enantiomeric conversion of **1–3** and **6**, but only a ring rotation accounts satisfactorily for this conversion in the case of **5**, and only a twist process accounts for the isomerization of **A** to **D**. No information is obtained about the nature of the twist, since the various types of twists proposed differ mainly only in the symmetry of the transition state [20] and give the same isomers. For compounds **1–3**, the presence of diastereoisomers is detected neither by ^1H NMR nor, more surprisingly by ^{13}C NMR spectroscopy. Very little information is available in this case since no decoalescence of the signals is observed above the melting point of the solvent.

Acknowledgements

The authors thank Professor J. Lapasset, Groupe de Dynamique des Phases Condensées, UA au CNRS nr. 233, Professor J. Rozière and I. Brach, Laboratoire des Acides Minéraux, UA and CNRS nr. 79, Université des Sciences et Techniques du Languedoc, and Professor C.G. Kreiter, Universität Kaiserslautern for helpful discussions. A N.A.T.O. Grant is gratefully acknowledged.

References and notes

1 G.T. Burns, E. Colomer and R.J.P. Corriu, Organometallics, 2 (1983) 1901.
2 G.T. Burns, E. Colomer, R.J.P. Corriu, M. Lheureux, J. Dubac, A. Laporterie and H. Houghmane, Organometallics, in press.

3 R.J. McMahon, Coord. Chem. Rev., 47 (1982) 1.
4 E.W. Abel, T. Blackmore and R.J. Whitley, J. Chem. Soc., Dalton Trans., (1976) 2484.
5 F. Carré, E. Colomer, J.Y. Corey, R.J.P. Corriu, C. Guérin, B.J.L.Henner, B. Kolani and W.W.C. Wong Chi Man, Organometallics, 5 (1986) 910.
6 C. Guimon, G. Pfister-Guillouzo, J. Dubac, A. Laporterie, G. Manuel and H. Iloughmane, Organometallics, 4 (1985) 636.
7 K.W. Muir, R. Walker, E.W. Abel, T. Blackmore and R.J. Whitley, J. Chem. Soc., Chem. Commun., (1975) 698.
8 D.T. Cromer and J.B. Mann, Acta Cryst., A 24 (1968) 321.
9 E. Colomer, R.J.P. Corriu and M. Lheureux, to be published.
10 H. Günther, NMR Spectroscopy, John Wiley and Sons, New York, 1980, pp. 240–244.
11 C.G. Kreiter, M. Kotzian and G. Ozkar, unpublished results and personal communication.
12 No atom is lying more than 0.004 Å apart from the least-squares mean plane.
13 G.E. Herberich, B. Hessner, E. Colomer and M. Lheureux, J. Organomet. Chem., submitted.
14 F. Carré, R.J.P. Corriu, C. Guérin, B.J.L. Henner, B. Kolani and W.W.C. Wong Chi Man, J. Organomet. Chem., 328 (1987) 15.
15 L.C. Ananias de Carvalho, M. Dartiguenave, F. Dahan, Y. Dartiguenave, J. Dubac, A. Laporterie, G. Manuel and H. Iloughmane, Organometallics, 5 (1986) 2205.
16 J.J. Fortman and R.E. Sievers, Coord. Chem. Rev., 6 (1971) 331.
17 N. Serpone and D.G. Bickley, Progr. Inorg. Chem., 17 (1972) 391.
18 L.H. Pignolet, Top. Curr. Chem., 56 (1975) 91.
19 C.G. Kreiter, Adv. Organomet. Chem., 26 (1986) 297.
20 R.S. Michalak, S.R. Wilson and J.C. Martin, J. Amer. Chem. Soc., 106 (1984) 7529.
21 J.C. Bailar, J. Inorg. Nucl. Chem., 8 (1958) 165.
22 P. Rây and N.K. Dutt, J. Indian Chem. Soc., 20 (1943) 81.
23 C.S. Springer Jr. and R.E. Sievers, Inorg. Chem., 6 (1967) 852.
24 G. Michael and C.G. Kreiter, Z. Naturforsch. B. 39 (1984) 1738 and preceeding papers.